JOURNAL OF VIROLOGY, Feb. 2010, p. 1856–1866 Vol. 84, No. 4
0022-538X/10/$12.00 doi:10.1128/JVI.02640-08

Rotavirus Infection Activates Dendritic Cells from Peyer's Patches in Adult Mice▽†

Delia V. Lopez-Guerrero,[1,2] Selene Meza-Perez,[5,6] Oscar Ramirez-Pliego,[3] Maria A. Santana-Calderon,[3] Pavel Espino-Solis,[2] Lourdes Gutierrez-Xicotencatl,[4] Leopoldo Flores-Romo,[5] and Fernando R. Esquivel-Guadarrama[1]*

Facultad de Medicina, Universidad Autonoma del Estado de Morelos, 62210, Morelos, Mexico[1]; Instituto de Biotecnologia, Universidad Nacional Autonoma de Mexico, 62210, Morelos, Mexico[2]; Facultad de Ciencias, Universidad Autonoma del Estado de Morelos, 62210, Morelos, Mexico[3]; Centro de Investigaciones Sobre Enfermedades Infecciosas, Instituto Nacional de Salud Publica, 62211, Morelos, Mexico[4]; Departamento de Biologia Celular, CINVESTAV-IPN, 07360, Mexico D.F., Mexico[5]; and Departamento de Inmunologia, Escuela Nacional de Ciencias Biologicas-IPN, 11340, Mexico D.F., Mexico[6]

Received 22 December 2008/Accepted 19 November 2009

This study used an *in vivo* mouse model to analyze the response of dendritic cells (DCs) in Peyer's patches (PPs) within the first 48 h of infection with the wild-type murine rotavirus EDIM ($EDIM_{wt}$). After the infection, the absolute number of DCs was increased by 2-fold in the PPs without a modification of their relative percentage of the total cell number. Also, the DCs from PPs of infected mice showed a time-dependent migration to the subepithelial dome (SED) and an increase of the surface activation markers CD40, CD80, and CD86. This response was more evident at 48 h postinfection (p.i.) and depended on viral replication, since DCs from PPs of mice inoculated with UV-treated virus did not show this phenotype. As a result of the activation, the DCs showed an increase in the expression of mRNA for the proinflammatory cytokines interleukin-12/23p40 (IL-12/23p40), tumor necrosis factor alpha (TNF-α), and beta interferon (IFN-β), as well as for the regulatory cytokine IL-10. These results suggest that, a short time after rotavirus infection, the DCs from PPs play a critical role in controlling the infection and, at the same time, avoiding an excessive inflammatory immune response.

Rotavirus (RV) is the most common cause of infectious diarrhea, killing almost 600,000 children globally each year, mainly in developing countries (35). RV belongs to the *Reoviridae* family and contains a genome composed of 11 segments of double-stranded RNA (dsRNA) that code for six structural (VP) and six nonstructural (NSP) proteins. RV tissue tropism *in vivo* is very specific, typically infecting only enterocytes on the tips of the intestinal villi of several animal species, including humans (26). However, RV infection also can induce antigenemia and viremia in blood and other tissues in humans and animal models (6, 7). The health impact of this viral disease has made the development of effective protective vaccines an international priority (36) that requires more knowledge regarding the *in vivo* immune responses against this virus.

Studies describing the immune mechanisms involved in protection against RV have been performed mainly in an established murine model of infection, using both homologous and heterologous viral strains. It has been shown that immunoglobulin A (IgA) participates in containing and clearing a primary infection and in the prevention of a secondary infection (10, 24). It also has been determined that cytotoxic T cells (Tc) are important in terminating the infection through mechanisms independent of Fas, perforin, and gamma interferon (IFN-γ), and that helper T cells (Th) are important in inducing efficient T-cell and B-cell responses through the secretion of cytokines (17, 28).

The balance between tolerance and inflammatory responses in the intestinal mucosa seems to be determined by characteristics of the microorganism, such as its life cycle, target cells, and pathogen-associated molecular patterns (PAMPs), and the expression of pattern recognition receptors (PRRs), including Toll-like receptors (TLRs) that are of particular importance during viral infections (5, 19). These molecules are present mainly in cells of the innate immune response. Among them, DCs play a crucial role in the induction of the innate immune response and are the most efficient antigen-presenting cells (APCs), inducing acquired responses by T cells and B cells; therefore, DCs are considered the link between the innate immune response and the acquired immune response (19, 43). The intestinal DCs are found along the different lymphoid compartments associated with the intestinal mucosa, both in inductive sites such as PPs and the mesenteric lymph node (MLN), where they capture potentially pathogenic antigens and are crucial in the induction of an effective immune response (19, 21, 33), as well as in the lamina propria (LP), which is considered the mucosal effector site (19, 34).

PPs and the MLN have a high concentration of naive T cells and B cells that are subject to activation by antigen-loaded DCs. The luminal antigens are transported to the subepithelial dome (SED) of the PPs by specialized cells called M cells,

* Corresponding author. Mailing address: CIQ, Laboratory-12, Universidad Autonoma del Estado de Morelos, Av. Universidad 1001, Col. Chamilpa, Cuernavaca, Morelos, 62210, Mexico. Phone: (52) (777) 3-29-70-00, ext. 3484. Fax: (52) (777) 3-29-70-48. E-mail: fernando.esquivel@uaem.mx.

† Supplemental material for this article may be found at http://jvi.asm.org/.

▽ Published ahead of print on 9 December 2009.

which are present in the follicle-associated epithelium (FAE) of the PPs (31, 32). At the SED, antigens are taken up by DCs, which subsequently acquire a mature phenotype characterized by the upregulation of CD40, CD80, and CD86 surface activation markers. These activation markers act as costimulatory molecules that are required for the efficient activation of T cells located in the interfollicular region. It has been suggested that DCs also activate B cells through a T-cell-independent mechanism (43). As a result of the stimulation by DCs in PPs and MLN, T and B cells express the intestinal homing receptor $\alpha4\beta7$ on their surfaces, which enables them to interact with the mucosal addressin cell adhesion molecule 1 (MAdCAM-1) that is present in the LP (23).

The role of the innate immune response against RV has been studied using *in vitro* models of human, simian, and mouse cells. These studies have shown that RV can induce the activation of the immune cells along with the release of various cytokines (18, 30). Sestak et al. showed that macaque monocyte-derived DCs present RV antigens to lymphocytes (41). This finding indicates that DCs are involved not only in antigen trapping but also in the active antigen presentation of RV particles to T cells. Likewise, using cells derived from human monocytes, it was found that mature DCs (MDCs) and immature DCs (IDCs) are able to interact with RV. Moreover, the IDCs treated with RV induce a proinflammatory response by strongly stimulating naive allogeneic $CD4^+$ T cells to secrete Th1 cytokines (30).

It has been discovered recently, using murine bone marrow DCs (bmDCs), that although infectious live virus and noninfectious virus-like particles (VLPs) are internalized by bmDCs and are able to induce the production of TNF-α, only infectious virus particles were able to induce the upregulation of the activation marker CD86 on these cells. It also was shown that diverse viral antigen elements (e.g., dsRNA) are capable of inducing the activation of bmDCs (18, 27).

In vitro studies of epithelial cells, fibroblasts, and bmDCs infected with RV suggest that this virus can evade the innate immune response by blocking the type I interferon (IFN) pathway (specially in epithelial cells and fibroblasts) (4, 13). This effect has been linked to the degradation of type I IFN transcription factors (IRFs) *via* their association with NSP1, a viral protein generated during viral replication. However, this mechanism has not been demonstrated *in vivo*.

Although *in vitro* studies of the interaction of DCs with RV have generated valuable information, it is important to analyze the role of intestinal DCs in the *in vivo* immune response against RV. In this study, we analyzed the activation status of DCs in the PPs of mice infected with the RV homologous murine strain $EDIM_{wt}$ during the first 48 h postinfection (p.i.). We found that, after infection, the DCs increased in absolute number and were mobilized to the SED of the PPs. This response correlated with an increase in the expression of the DC surface activation markers CD40, CD80, and CD86, as well as in the mRNA expression of IL-10, IFN-β, IL-12/23p40, and TNF-α genes. Finally, it was found that the activation of the DCs was dependent on viral replication. These results show that shortly after RV infection, the DCs from PPs have a mixed immune response, which suggests that they play an important role in controlling the infection through the production of antiviral cytokines and the priming of T cells and, at the same time, avoiding an excessive inflammatory immune response.

MATERIALS AND METHODS

Animals. Pathogen-free, 4- to 8-week-old adult female BALB/c mice ($H\text{-}2^d$) were provided by the Biotechnology Institute (IBT, UNAM) and the National Institute for Public Health (INSP, SSA), Cuernavaca, Morelos, Mexico. Animals were housed under standard natural lighting conditions (12 h light/12 h dark) and were given food and water *ad libitum*. Previous RV infection was ruled out by the absence of RV-specific serum antibodies (Abs) as determined by enzyme-linked immunosorbent assay (ELISA).

Virus. Murine RV $EDIM_{wt}$ (Mu/G3P10), kindly donated by Richard Ward (Children's Hospital Medical Center, Cincinnati, OH), was grown *in vivo* in neonatal mice (3 to 5 days old) (50). Pups were orally infected, and the intestines were collected 72 h later to generate homogenates in TNC (10 mM Tris, 100 mM $NaCl_2$, 1 mM $CaCl_2$; pH 7.4). Aliquots of the homogenates were stored at −80°C until use. The 50 infectious dose (ID_{50}) *in vivo* was determined using infected adult mice as previously described (9). Infectivity *in vitro* was determined in the MA-104 cell line (a rhesus monkey kidney cell line) by the immunoperoxidase focus assay described below.

Virus inactivation. Intestinal homogenates of RV $EDIM_{wt}$ were inactivated using UV short-wave treatment. Briefly, intestinal homogenates were suspended in phosphate-buffered saline (PBS) at a final virus concentration of 10^4 focus forming units (FFU)/100 μl, and psoralen (Sigma) was added to a final concentration of 40 μg/ml. The mixture was placed on ice and UV irradiated for 30 min at a distance of 10 cm from the source (Lamp, UVP Inc., San Gabriel, California). This treatment reduced the *in vitro* infectivity of the virus up to 95% as assessed by the immunoperoxidase focus assay.

Titration of viral RV $EDIM_{wt}$ *in vitro* by immunoperoxidase focus assay. The immunoperoxidase focus assay was performed by a modified version of a standard method described previously (2). Briefly, MA-104 cells were seeded into 96-well plates at a density allowing the monolayers to reach confluence for 2 to 3 days. The monolayers were incubated in serum-free medium for 16 to 18 h and inoculated with serial 10-fold dilutions of trypsin-activated virus (100 μl/well). The viral inoculum was prepared by incubating virus stocks (intestinal homogenate) with 5 μg/ml trypsin for 30 min at 37°C. The plates with the inoculum were incubated at 37°C for 1 h, with occasional rocking to allow virus adsorption. After being washed with PBS, the plates were incubated at 37°C for 1 h with a rabbit polyclonal hyperimmune antiserum against triple-layer particles (TLPs) of porcine RV YM (1:1,000) (kindly provided by Carlos Arias, IBT, UNAM, Mexico). Following incubation, the plates were washed twice with PBS and incubated at 37°C for 1 h with a goat anti-rabbit immunoglobulin G (IgG) antibody (Ab) coupled to peroxidase (Santa Cruz) (1:2,500) using the peroxidase substrate 3-amino-9-ethylcarbazole (Sigma). Finally, cells with brown precipitate were counted under a light microscope Nikon Eclipse TE300 (Nikon Inc., Tokyo, Japan), and the number of FFU/ml was calculated.

Mouse infection. Groups of four animals of 4- to 8-week-old adult female BALB/c mice were inoculated orally with the murine RV $EDIM_{wt}$. First, gastric acid was neutralized by administering 100 μl of 1.3% sodium bicarbonate by proximal esophageal intubation. After 10 min, the mice were inoculated with 100 μl of serum-free MEM containing 1×10^4 FFU of the virus (100 times the ID_{50}) or, as control, with 100 μl of medium alone. Stool samples were collected daily up to day 3 or 8 p.i. and frozen at −20°C. The viral load in the stools was determined by plate ELISA, as described below.

Detection of RV antigen in stools by ELISA. Murine stool samples were incubated overnight at 4°C in dissociating buffer (TNC, 5% fetal calt serum (FSC), 0.05% Tween-20, 1.4 mM sodium azide), disaggregated by vortexing, and centrifuged at 13,000 rpm, and the supernatant was recovered. The viral load in the supernatant was evaluated by ELISA in a 96-well plate format (Costar high-binding) by coating with goat anti-RV hyperimmune serum (made in our laboratory) diluted 1:5,000 in PBS. Plates were incubated overnight at 4°C and blocked with 5% (wt/vol) Carnation nonfat milk in TNC at room temperature (RT) for 2 h. Supernatants were added to the wells and incubated for 2 h at 37°C. The plates were washed four times with the wash solution (TNC, 0.2% Tween 20), and rabbit anti-RV polyclonal hyperimmune serum (made in our laboratory) diluted 1:2,000 was added and incubated for 1 h at 37°C. After four washes, a goat anti-rabbit IgG Ab coupled to alkaline phosphatase (Zymed) was added and incubated for 1 h at 37°C. The substrate (*p*-nitrophenyl phosphate, disodium; Sigma) was added, and the plates were developed for 30 to 45 min at 37°C. The absorbance at 405 nm was read with a plate reader (Labsystem, Original Multiskan).

Immunohistochemistry of PPs. Groups of four adult female BALB/c mice were inoculated orally with 10^4 FFU of the murine RV $EDIM_{wt}$ or UV-inactivated RV $EDIM_{wt}$. The animals were sacrificed by cervical dislocation at 0, 12, 24, or 48 h p.i. The small intestines were excised through an abdominal incision and washed with cold saline solution (150 mM NaCl). PPs were collected in petri dishes containing saline solution, and the tissues were embedded in Jung tissue freezing medium (Leica Microsystems, Nussloch, Germany), immediately frozen in liquid nitrogen, and stored at −80°C until use. Samples were cut into 6-μm frozen sections using a Leica 1850CM cryostat (Nussloch, Germany) and fixed in cold acetone-chloroform (1:1) for 20 min. To block endogenous peroxidase activity, the sections were treated with 9% H_2O_2 in PBS for 1 h at RT and washed in PBS containing 0.1% bovine serum albumin (BSA). Before specific Ab staining, nonspecific binding was blocked with 2% rabbit serum in PBS for 1 h at RT. To detect DCs, 100 μl of PBS containing 1 μg of purified hamster anti-mouse CD11c monoclonal Ab (MAb) (clone N418; kindly provided by Lourival Possani, IBT, UNAM, Mexico) were added to the samples. After overnight incubation at 4°C, the samples were washed twice with PBS–0.5% BSA and incubated with goat anti-hamster IgG Ab coupled to peroxidase (eBioscience) (1:500) in the same buffer for 1 h at RT. After three washes, chromogen substrate (3-amino-9-ethylcarbazole; Sigma) was added, and the samples were developed for 10 min at RT. Samples were washed extensively with distilled water and counterstained with hematoxylin-eosin or 5% methyl green (Sigma) in methanol and rinsed with distilled water, and the slides were mounted in 60% glycerol PBS and analyzed under a light microscope (Eclipse TE300; Nikon Inc., Tokyo, Japan).

Immunofluorescence of PPs. Groups of four adult female BALB/c mice were inoculated orally with 10^4 FFU of murine RV $EDIM_{wt}$. The animals were sacrificed by cervical dislocation at 0 and 48 h p.i., and PP samples were collected as described above. Before specific Ab staining, nonspecific binding was blocked with 2% human serum in PBS containing 0.5% BSA and 0.05% Triton X-100 (Affimetrix-USB) for 1 h at RT. To detect RV NSP5, 100 μl of PBS–0.5% BSA–0.05% Triton X-100 containing 4 μl of polyclonal rabbit anti-NSP5 (1:25) (kindly provided by Susana López, IBT, UNAM, Mexico) and 2 μl of rat MAb anti-CD11c coupled to fluorescein isothiocyanate (FITC) (BD Bioscience) (1:50) were added to each sample. After overnight incubation at 4°C with the Abs, the samples were washed three times with PBS–0.5% BSA–0.05% Triton X-100 and incubated with goat anti-rabbit IgG Ab coupled to Alexa 568 (Molecular Probes) (1:100) in the same buffer for 1 h at RT (protected from light). Samples were washed extensively with PBS–.1% BSA–0.05% Triton X-100 and incubated for 10 min with 4′,6-diamidino-2-phenylindole, dihydrochloride (DAPI) (Molecular Probes); afterward the slides were washed with PBS and mounted in 60% glycerol PBS. The samples were analyzed by epifluorescence microscopy (Zeiss Axiovert 200 M), and images were taken with an Axiocam MRM using Axiovision 3.1 software (Carl Zeiss, Inc.).

Isolation of total cells from PPs. PPs were removed from the small intestine and washed three times with saline physiologic solution. PPs were digested for 20 min at 37°C in Hank's medium containing 0.150 μg/ml collagenase VIII (Sigma), 5 μg/ml DNase (Sigma), 5% fetal bovine serum, and 5 mM EDTA using gentle agitation. PPs were mechanically dissociated through a metallic sieve (Sigma-Aldrich). The cellular suspension was centrifuged at 1,700 rpm for 10 min at 4°C. The cell pellet then was resuspended in Hanks' balanced salt solution (without Ca^{2+} and Mg^{2+}). Viable cells were counted in a Neubauer chamber by the trypan blue exclusion method.

DCs enriched from PPs by flotation through a low- density gradient. The cell suspension obtained after enzymatic digestion and mechanical disaggregation was loaded onto an OptiPrep (Axis-Shield, Oslo, Norway) gradient (1.077 to 1.080 g/ml) according to the manufacturer's recommendations (C-20 application sheet). The DC-enriched band was extracted by aspiration, analyzed by flow cytometry, and purified by positive selection as described below.

Purification of DCs from PP. The DC-enriched cell fraction obtained by the OptiPrep density gradient was used for DC purification by positive selection using magnetic-activated cell sorting (MACS). DC-enriched cells obtained by density gradient were suspended in PBS, 0.5% BSA, 2 mM EDTA (MACS buffer), and Fc receptors (FcgRIII/II) were blocked using 1 μg of anti-mouse MAb CD16/CD32 (eBiosciences). DCs from PPs were purified by positive selection using anti-mouse CD11c-coated magnetic bead Ab (clone N418) (Miltenyi Biotech, Auburn, CA) for 20 min at 4°C. The samples were rinsed and selected on MACS separation columns according to the manufacturer's recommendations. The purity was verified by flow cytometry using anti-mouse CD11c-allophycocyanin (CD11c-APC), TCR-FITC, CD11b-phycoerythrin (CD11b-PE), B220-FITC (BD Biosciences), biotinylated anti-F4/80 (Serotec) antibodies, and streptavidin coupled to Alexa 647 (Molecular Probes), obtaining an approximately 90% purity. The purified cells were used for conventional and real-time PCR cytokine analyses.

Flow cytometry. Cells were suspended in binding buffer (PBS, 0.5% BSA, 5 mM EDTA) and stained with the appropriate Ab. Before being stained, cells were incubated with Fc block anti-CD16/CD32 MAb for 15 min at 4°C. Cells were stained with the following anti-mouse MAbs purchased from BD Bioscience: CD11c-FITC (1:100), CD11c-APC (1:300), CD8-FITC (1:200), TCR-FITC (1:200), B220-FITC (1:300), biotinylated CD11c (1:100), biotinylated CD80 (1:200), CD11b-PE (1:100), and CD40-PE (1:100). Biotinylated CD40 (1:200), CD86-PE (1:200), and CD4-peridinin chlorophyll protein (PerCP) (1:300) were obtained from eBioscience. Biotinylated F4/80 (1:100) was provided by Serotec. Abs were added and incubated for 20 min at 4°C. Biotinylated Abs were detected using streptavidin-conjugated PerCP (1:400) (BD Biosciences) and streptavidin-conjugated Alexa 647 (1:800) (Molecular Probes). The MAb made in rat, anti-major histocompatibility complex class II (MHC-II) (NIM R4), was kindly donated by Vianney Ortiz (CINVESTAV, Mexico), and the MAb anti-CCR6 was kindly donated by Eduardo Garcia (IIB-UNAM, Mexico), and they were detected with goat anti-rat IgG coupled to FITC (1:100) (Zymed). Appropriate isotype controls were included in all experiments. The cellular suspensions were fixed with 2% paraformaldehyde (Sigma-Aldrich). Cellular staining analysis was performed on a FACSCalibur (Becton Dickinson, Mountain View, California), acquiring 50,000 or 100,000 events for each experiment. Gating was done using FlowJo software (Tree Star, Inc.). Dead cells were discarded from analysis by propidium iodide staining (Invitrogen).

Analysis of mRNA expression for different cytokines in enriched DCs from PPs. Total RNA was isolated from 2×10^5 purified DCs obtained from PPs after MACS purification. The RNA was isolated using TRIzol (Invitrogen) by following the manufacturer's protocol. The integrity of the RNA was assessed by the visual analysis of 28S and 18S ribosomal RNAs after electrophoresis in a 1% agarose gel and staining with ethidium bromide. Subsequently, reverse transcriptions were performed from 500 ng of total RNA using the Revert Aid H Minus First Strand cDNA Synthesis kit (MBI Fermentas) with oligo(dT) according to the manufacturer's protocol. The mRNA expression of IFN-β and β-actin was assessed by conventional PCR using *Taq* DNA polymerase (MBI Fermentas) and 10× *Taq* buffer with $(NH_4)_2SO_4$ using the primers 5′-CCACAGCCCTCT CCATCAAC and 3′-TCTCTGCTCGGACCACCATC for IFN-β and 5′-ATG AGGTAGTCTGTCAGGT and 3′-ATGGATGACGATATCGCT for β-actin. The cDNA reaction mix was incubated in a MultiGene Gradient Thermal Cycler (Labnet) through initial denaturation at 92°C for 2 min, followed by 30 cycles of 1 min at 92°C, 1 min at 62°C, and 1 min at 72°C, and then a final extension at 72°C for 10 min. PCR products were analyzed on a 1.5% agarose gel, stained with ethidium bromide, and visualized on a UV transilluminator (BioDoc-It Imaging System). The mRNAs for IL-12/23p40, TNF-α, and IL-10 were analyzed using real-time PCR. For this, the cDNA was diluted 1/10, and 2 μl of the diluted sample was used for amplification in a 5700 Gene Amp (Applied Biosystems) with 15-min denaturation and 1-min annealing/extension cycles, and expression was normalized against the 18S rRNA gene. We used the PDAR designed reagents for the TaqMan amplification of the cytokines (Applied Biosystems). All of the primers have equivalent melting temperatures and give amplicons of 100 to 120 bp.

Statistical analysis. Statistical significance was evaluated using the t-Student's *t*-test in SPSS 17.0 software with a confidence interval of 99%.

RESULTS

The number of DCs in PPs of infected mice increases during RV infection. We used an adult mouse model of RV infection to analyze the response of DCs from PPs. In this model, mice infected orally with the murine RV $EDIM_{wt}$ present a shedding kinetic that initiates on day 2 and terminates on day 8 (see Fig. 2D). During the course of this study, we analyzed the PP DCs from the jejunum and ileum, but as both intestinal regions gave similar results, only results of the experiments with PPs from jejunum are shown. We first determined whether the total DC number in PPs from RV-infected mice increased during the first 48 h p.i., since it is well known that PPs suffer hyperplasia and an increase in the total cell number as a result of this infection (8). Thus, PPs cells from infected and control mice were isolated at 0 (control, noninfected mice) and at 24 h and 48 h p.i., and the cells were counted using the trypan blue exclusion method. It was found that the total cell number of

PPs of infected mice showed a significant increase ($P < 0.05$) compared to that of the noninfected control mice at both 24 and 48 h p.i. (see Fig. S1A in the supplemental material).

To analyze the percentage and absolute number of DCs and other cell populations, the total cells from PPs were analyzed by flow cytometry using MAbs specific for CD11c, CD4, CD8, CD11b, and B220. We found that, compared to noninfected mice, infected mice showed a significant increase ($P < 0.05$) in the absolute number of PP DCs (2-fold at 48 h p.i.) (Fig. 1A), but with no significant difference in their percentage (approximately 4.5% in all cases; data not shown). The other cell populations analyzed did not show a significant change in the percentage after infection either, but $CD4^+$, $CD11b^+$, and $B220^+$ cells had an increase in their absolute number at 48 h p.i. (see Fig. S1B and C in the supplemental material). It is important to point out that $B220^+$ cells are the predominant cell population of PPs (60%) and the one that showed the highest increment in their absolute number, as has been shown previously (8). These results suggest that after RV infection the PPs, among other cell populations, have an influx of DCs that contribute to the immune response.

To further characterize the phenotype of the $CD11c^+$ cells, total cells from PP at 0 and 48 h p.i. were costained with anti-CD11c, MHC-II, and F4/80 MAbs. The expression of MHC-II in CD11c cells is an important marker for DCs (46), but F4/80 is a marker of macrophages only when expressed at high levels (37, 47). Previous studies have reported the expression of F4/80 in CD11c cells from PPs and other lymphoid organs, but at low levels (38, 47). It was found that at 0 h, 87.65% ± 4.95% of $CD11c^+$ cells were MHC-II^+, 14.5% ± 3.2% were F4/80^{low}, and 20.7% ± 4.3% were MHC-II^+ F4/80^{low}. On the other hand, at 48 h p.i., 88.49% ± 3.15% of $CD11c^+$ cells were MHC-II^+, 16.5% ± 1.3% were F4/80^{low}, and 22.5 ± 2.4% were MHC-II^+ F4/80^{low}. These results show that most of $CD11c^+$ cells analyzed in the total cell population from PPs exhibit a DCs phenotype and do not contain a significant number of cells with a macrophage phenotype ($CD11c^{low}$ F4/80^{high}) (22, 37, 47).

RV infection induces the mobilization of DCs to the SED of PPs. We determined the effect of the RV infection on the distribution of PP DCs from the jejunum and ileum. Cryosections of PPs were obtained at 0, 12, 24, and 48 h p.i., and the DCs were detected by immunoperoxidase staining using a purified hamster anti-mouse CD11c MAb. The PP DCs from noninfected mice were distributed in the whole area of this lymphoid organ, including the SED and the interfollicular region (IFR). At 24 h p.i. the DCs initiated migration toward the SED, and at 48 h p.i. the majority of these cells were lined up in this region (Fig. 1B). This result shows that the RV infection induces a complete mobilization of DCs toward the SED within the first 48 h p.i.

To evaluate whether PP cells, and in particular $CD11c^+$ cells, can be infected by RV at early times after RV administration, PPs from jejunum of noninfected and mice infected for 48 h were removed and cryopreserved. Frozen sections of PPs were stained with FITC-conjugated anti-CD11c MAb and rabbit anti-RV NSP5 polyclonal hyperimmune serum (NSP5 is synthesized only during viral replication) and analyzed by epifluorescence microscopy. It was found that PPs presented less than 1% of cells expressing NSP5, with no evident colocalization with $CD11c^+$ cells (see Fig. S2C and D in the supplemental material). In contrast, epithelial cells on the intestinal villi (adjacent to PP) showed a clear signal for NSP5 (see Fig. 2A and B in the supplemental material). This result indicates that at early times after RV inoculation, the infection takes place almost exclusively in epithelial cells located in the apex of the intestinal villi.

It has been shown that the mobilization of DCs toward the SED of the PPs is due to the secretion of chemokines such as CCL20 by the FAE overlaying the dome region (52), allowing the DCs expressing CCR6 to receive antigens through the M cells, to mature, and to initiate an immune response. To correlate the mobilization of the DCs to the SED of PPs from infected mice with the expression of CCR6, total cells from PPs of noninfected mice and mice infected for 48 h were costained with MAbs specific for CD11c and CCR6 and analyzed by flow cytometry. It was found that DCs from PPs of noninfected mice expressed constitutive levels of the CCR6 molecule, whereas DCs from infected mice showed a slight increase in the expression of this molecule (Fig. 1C).

To determine the degree to which the induction of the mobilization of DCs depends on viral replication, mice were inoculated with RV $EDIM_{wt}$ attenuated by UV treatment. The UV treatment was performed in the presence of psoralen, which preserves the antigenic characteristics of the external proteins. The infectivity of EDIM was totally abrogated in the MA-104 cell line; however, some viral load in the feces of the mice could be detected at 72 h p.i., followed by an abrupt increase that reached levels similar to those of the nontreated virus by the fourth day, and as in the nontreated virus, the viral load declined by day 6 and disappeared by day 8 (Fig. 2D). During the first 48 h p.i. with UV-treated RV, there was not an evident migration of $CD11c^+$ cells toward the dome of the PPs (Fig. 2A to C), in contrast to results for nontreated RV-infected mice (Fig. 1B). This result indicates that the inoculated viral particles are not sufficient to induce the efficient migration of DCs to the SED of PPs, since viral replication and the increase of viral antigen in the lumen, as well as epithelial cell damage, may be crucial for the efficient activation of DCs.

Activation of DCs in PPs of infected mice. We tested whether the mobilization of the DCs after RV infection correlated with the level of surface expression of CD40, CD80, and CD86 activation markers. To this end, at 0, 24, and 48 h p.i. cells from PPs were centrifuged through a low-density gradient (1.077 to 1.080 g/ml) of OptiPrep. This procedure enriches the DCs population (38) and eliminates most of the macrophages, since they require higher density for purification (22). The DC-enriched band was obtained, and cells were stained with anti-mouse CD11c, MHC-II, CD40, CD80, or CD86 MAb and analyzed by flow cytometry. The analysis of the activation markers was performed on cells in the $CD11c^+$ MHC^+ gate (Fig. 3A). The percentage of DCs obtained in the enriched population was from 12 to 17%, compared to approximately 4.5% of the total cell population. The number of DCs recovered after the gradient corresponded to almost 99% (for 0 and 24 h) and 87% (for 48 h) of the original absolute number of DCs. On the other hand, the mean fluorescent intensity (MFI) of the activation markers increased after 48 h p.i. on DCs (Fig. 3A and B). The increase of the markers correlated with the abrupt increase in the viral load present in the feces

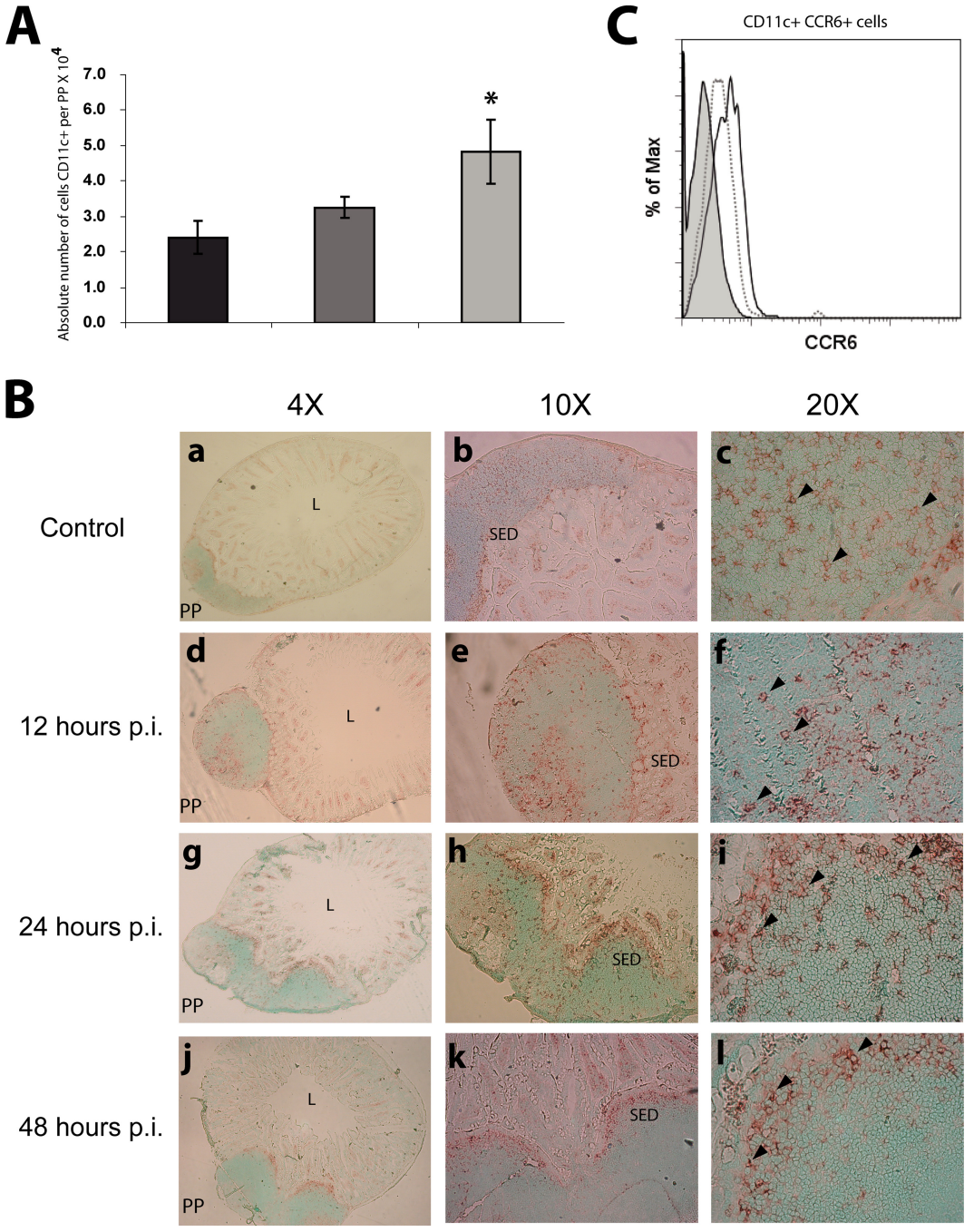

FIG. 1. After RV infection, DCs in PPs increase their absolute number and migrate to the SED. Groups of four mice were inoculated orally with 10^4 FFU of the murine RV $EDIM_{wt}$. Total cells from PPs of the small intestine were obtained from RV $EDIM_{wt}$-infected mice after 0 (control mice), 24 and 48 h p.i.; stained with rat anti-mouse CD11c and CCR6 MAbs; and analyzed by flow cytometry. (A) The absolute number of DCs was calculated by multiplying the percentage of DCs by the total cell number per PP. Shown are cells from noninfected mice (black bars) and from RV-infected mice 24 (gray bars) and 48 h p.i. (light gray bars). Bars represent the standard deviations. An asterisk indicates significant difference with respect to the control ($P < 0.05$, Student's t test). (B) PP from jejunum were obtained from mice at 0, 12, 24, and 48 h p.i. and cryopreserved. The frozen sections of the PPs were stained with the MAb hamster anti-mouse CD11c (clone N418) and developed with a secondary goat anti-hamster IgG Ab coupled to peroxidase using 3-amino-9-ethylcarbazole chromogen substrate. (a, b, c) Histological analysis of $CD11c^+$ cells in PPs of noninfected mice. (d, e, f) $CD11c^+$ cells in PPs at 12 h p.i. (g, h, i) $CD11c^+$ cells in PPs at 24 h p.i. (j, k, l) $CD11c^+$ cells in PPs at 48 h p.i. Arrows indicate $CD11c^+$ cells. L, intestinal lumen; SED, subepithelial dome. The experiment has been repeated with similar results with at least 30 PPs of jejunum and ileum. (C) Histogram of CCR6 MFI of $CD11c^+$ cells from PPs. Isotype control (light gray histogram), cells from noninfected mice (dotted line), and cells from RV-infected mice at 48 h p.i. (solid line) are shown. The histogram is respresentative of three independent experiments.

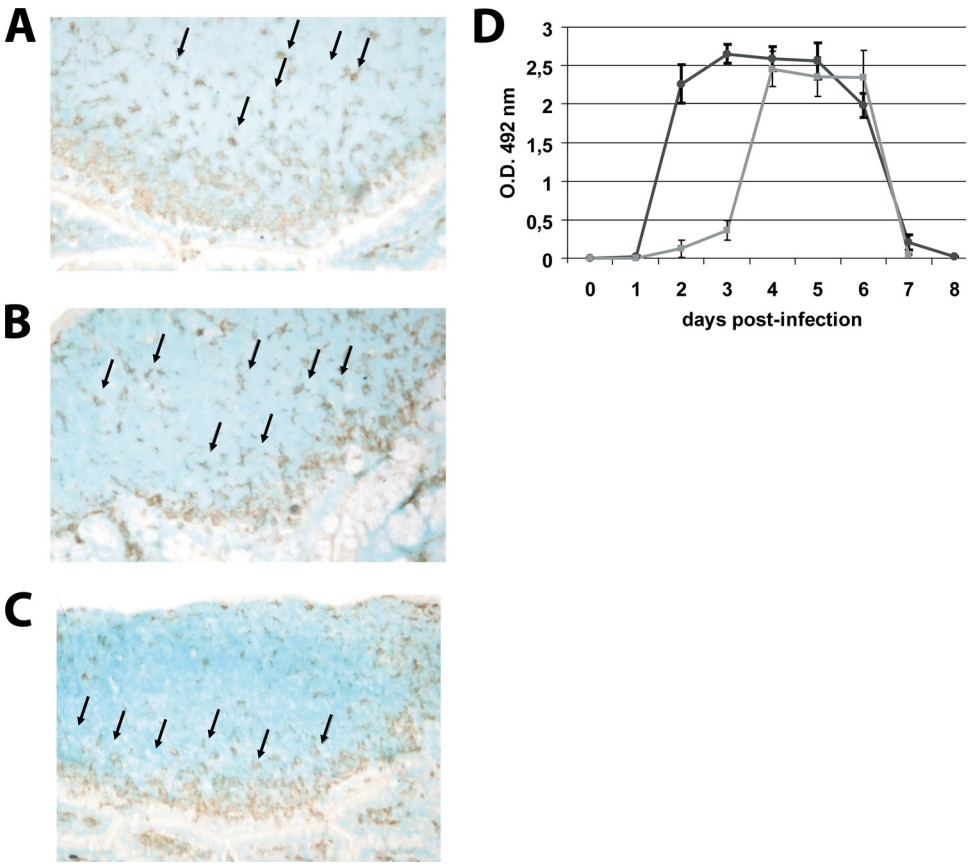

FIG. 2. UV-treated virus did not induce the migration of DCs to the SED of PPs. PP from jejunum of RV $EDIM_{wt}$-infected mice or from mice inoculated with UV-treated virus were obtained and cryopreserved at 0 (control mice) and 48 h p.i. The frozen sections of the PPs were stained with a CD11c-specific hamster MAb (clone N418) and developed with a secondary goat anti-hamster IgG Ab coupled to peroxidase using 3-amino-9-ethylcarbazole chromogen substrate. (A) Histological analysis of $CD11c^+$ cells in PPs of noninfected mice. (B) $CD11c^+$ cells in PPs at 48 h p.i. with UV-treated virus. (C) $CD11c^+$ cells in PPs at 48 h p.i. with infectious RV. Arrows indicate $CD11c^+$ cells. For panels A, B, and C a representative picture from 30 PPs is shown. (D) RV shedding curves. Groups of four mice were inoculated orally with 10^4 FFU of murine RV $EDIM_{wt}$ (dark gray line) or UV-treated RV $EDIM_{wt}$ (light gray line). Fecal rotavirus antigen was measured from day 0 to 8 by ELISA, and the results were expressed as the net optical density (O.D.) value. Bars represent the SD. The data shown are representative of three independent experiments.

(Fig. 2D), which suggests that the induction of the activation markers is dependent on viral replication. Accordingly, DCs from PPs from mice inoculated with UV-treated virus (see above) did not show a significant increase in the expression of the activation markers (Fig. 3C).

RV infection induces an increment in the mRNA synthesis for proinflammatory and regulatory cytokines in DCs from PPs. Intestinal DCs play a crucial role in initiating an immune response against incoming pathogens. Once they are activated, they secrete proinflammatory cytokines that can act to eliminate the pathogen directly or through the induction of an efficient adaptive immunity. As the DCs from PPs are activated and mobilized to the SED early in the course of the RV infection, we analyzed the level of mRNA for IFN-β, IL-10, IL-12/23p40, and TNF-α. Mice were infected with RV, and PPs were removed and disaggregated at 0 and 48 h p.i. In some experiments, samples at 24 h p.i. were obtained. The cell suspension was submitted to density gradient enrichment for DCs using OptiPrep medium. The enriched fraction then was used for DC purification by positive selection using the MACS protocol, obtaining a 90 to 93% purity for $CD11c^+$ cells that were 89% $MHC\text{-}II^+$, as assessed by flow cytometry (Fig. 4A). The residual cells were mainly T cells, with a marginal presence of $CD11c^-$ $CD11b^+$ and $CD11c^-$ $F4/80^+$ cells (data not shown). Total RNA from $CD11c^+$ and $CD11c^-$ cells was obtained using TRIzol and used for cDNA synthesis with oligo(dT). The mRNA for the IFN-β gene was analyzed by conventional PCR, and mRNA for IL-10, IL-12/23p40, and TNF-α was assessed by real-time PCR. It was found that at 48 h p.i., the DCs clearly express mRNA for IFN-β. In contrast, DCs from the control and $CD11c^-$ cells from both RV-infected and noninfected mice had undetectable IFN-β mRNA (Fig. 4B). On the other hand, a time-dependent increase of the mRNA for IL-10, IL-12/23p40, and TNF-α was observed between 24 and 48 h p.i. (Fig. 4C). At 48 h p.i. there was a 12- and 8-fold increase in the mRNA of the proinflammatory cytokines IL-12/23p40 and TNF-α, respectively, compared to levels for the noninfected control, and a 19-fold increment in the mRNA of the regulatory cytokine IL-10. The $CD11c^-$ cells from infected mice, assayed only at 0 and 48 h p.i., showed an increase of 2.5- and

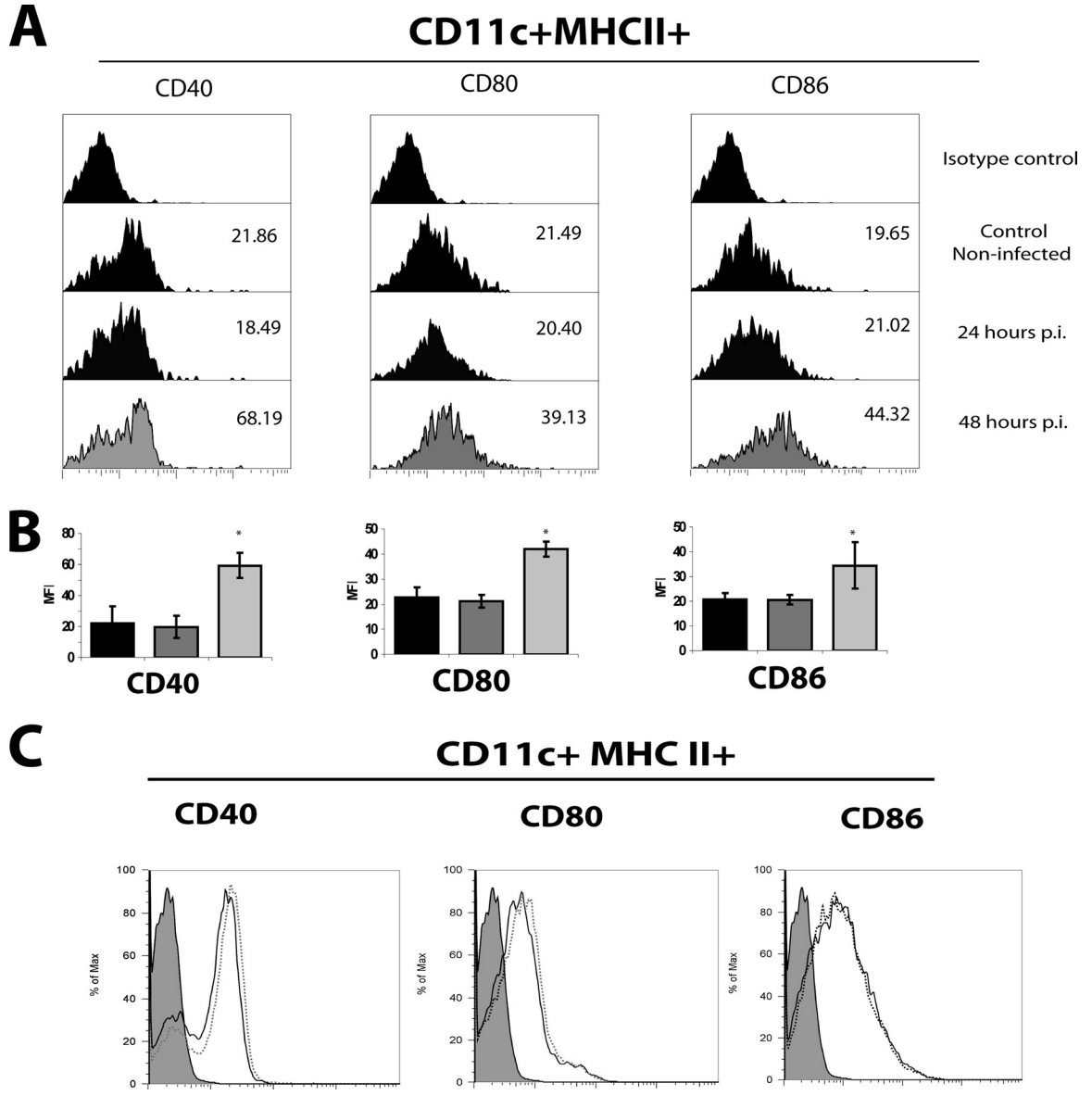

FIG. 3. RV infection induces the activation of DCs in PPs. Groups of five mice were inoculated orally with 10^4 FFU of murine RV $EDIM_{wt}$ or UV-treated RV. At 0 (control mice), 24, and 48 h p.i., the PPs from jejunum were obtained and dissociated. Total cells from PPs were DC enriched by centrifugation using OptiPrep medium. The DC-enriched fraction was stained for CD11c, MHC-II, CD40, CD80, and CD86 and analyzed by flow cytometry. (A) Histograms of the expression of CD40, CD80, and CD86 activation markers within the $CD11c^+$ $MHC\text{-}II^+$ gate in cells from noninfected and RV-infected mice. The data shown are representative of three independent experiments. (B) Summary of the data showed in panel A. MFI of cells from noninfected mice (black bars) and from RV-infected mice at 24 (gray bars) and 48 h p.i. (light gray bars) are shown. Isotype controls were used in each experiment. Bars represent the SD. The asterisk indicates significant difference with respect to the control ($P < 0.05$, Student's t test). (C) Histograms of the expression of CD40, CD80, and CD86 activation markers within the $CD11c^+$ $MHC\text{-}II^+$ gate in cells from noninfected and UV-treated RV-inoculated mice. Cells were from noninfected mice (dotted line) and mice infected 48 h p.i. (solid line). Gray histograms represent the isotype control. The data shown are representative of three independent experiments.

7-fold in the mRNA for TNF-α and IL-10, respectively, compared to levels for noninfected mice (Fig. 4D). No significant expression of IL-12/23p40 mRNA was detected in $CD11c^-$ cells from both infected and noninfected mice. It is clear from these results that the activation and mobilization of DCs to the SED of PPs from mice infected with RV correlates with the synthesis of both proinflammatory and regulatory cytokines produced by the DCs themselves and other cell types.

DISCUSSION

RV infects and replicates in the enterocytes present on the tips of the small intestinal villi. The infection induces both intestinal B-cell and T-cell protective responses that have been widely described previously (15, 16). However, only a few studies have addressed the role of the innate immune response in this infection (13, 18, 29, 30, 48, 51). Since DCs play a crucial role in the induction of innate and adaptive anti-viral re-

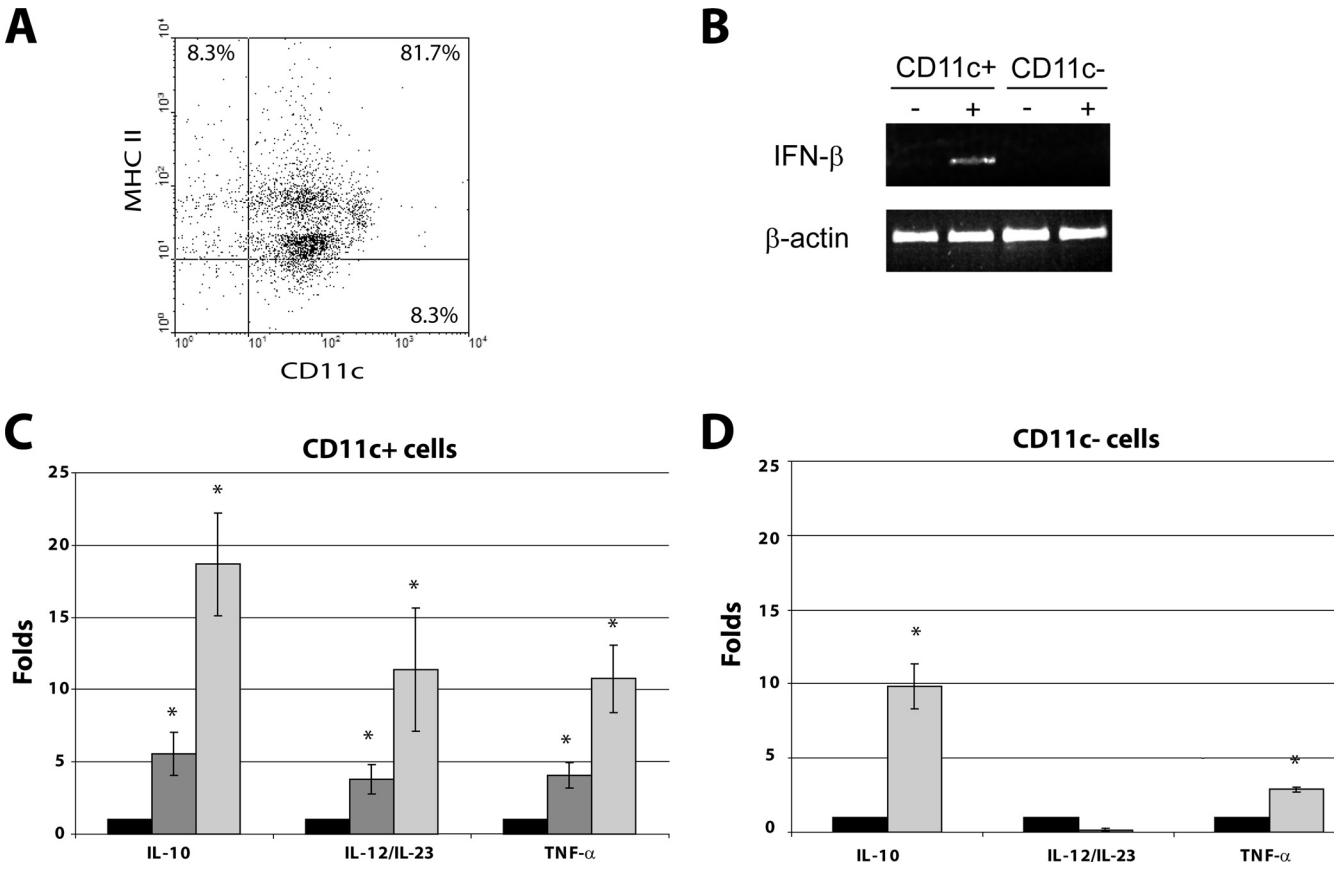

FIG. 4. RV infection induces the transcription of mRNA for different cytokines in DCs from PPs. Groups of five mice were inoculated orally with 10^4 FFU of the murine RV $EDIM_{wt}$, and the PPs from jejunum were obtained at 0, 24, and 48 h p.i. Total cells from PPs were DC enriched by centrifugation using OptiPrep medium, and $CD11c^+$ cells were positively selected using MACS. (A) Dot plot of purified cells from noninfected mice were stained with anti-CD11c and MHC-II MAbs and analyzed by flow cytometry. The data shown are representative of three different experiments. Similar results were obtained with cells from RV-infected mice. (B) mRNA from $CD11c^+$ and $CD11c^-$ cells from RV-infected mice at 48 h p.i. was amplified for the IFN-β gene by conventional PCR using specific primers. β-Actin mRNA was used as a constitutive message. +, sample from RV-infected mice; −, sample from noninfected mice. Fold increases for IL-10, IL-12/23p40, and TNF-α mRNA in purified $CD11c^+$ (C) and $CD11c^-$ (D) cells of RV-infected mice compared to levels for noninfected mice, as measured by real-time PCR. mRNA for ribosomal 18S proteins was used to normalize the level of the different mRNA. Noninfected mice (black bars) and RV-infected mice at 24 h p.i (gray bars) and 48 h p.i (light gray bars) are shown. Bars represent the standard errors. An asterisk indicates significant difference with respect to control ($P < 0.05$, Student's t test).

sponses, this study analyzed the response of DCs from PPs of adult mice infected with a murine wild-type RV strain. We found that during the first 48 h p.i. the DCs from PPs of infected mice increase in number, migrate to the SED, and upregulate the CD40, CD80, and CD86 surface activation markers, and that this response correlates to viral replication. Also, an increase in the mRNA expression for proinflammatory (IFN-β, IL-12/23p40, and TNF-α) and antiinflammatory (IL-10) cytokine genes was observed.

At 48 h p.i., there was an evident hyperplasia in PPs from the jejunum and the ileum that correlated with a significant increase in the total cell number. Similar results were described by Blutt et al. for mice infected with the murine RV strain EC_{wt} (8). They showed that although both T cells and B cells contributed to total cell number increment, the B-cell population was the predominant proliferating cell population, even in the absence of T cells (9). We also found that T cells and B cells, especially the latter, are responsible for the total cell number increase in PPs at 48 h p.i. (see Fig. S1 in the supplemental material). On the other hand, DCs also showed a significant increase in their absolute cell number without changes in the percentage of DCs at 24 and 48 h p.i. This suggests that early after infection, a significant influx of DCs from the circulation takes place in the intestinal PPs.

In recent work, Zhang et al. showed that the RV infection in neonatal gnotobiotic pigs induced the recruitment of monocytes/macrophages in the intestine (ileum) but not DCs, based on the cell percentage, which is in accordance with our results in PPs (51). Unfortunately, the absolute number in Zhang's study was not evaluated, so we cannot contrast this parameter with our work. However, it is very likely that at 5 days p.i. the pig's ileum suffers hypertrophy, as is seen in mice; therefore, the absolute number should be increased as well. Although there are important methodological differences between Zhang's work and ours (time of infection, analysis of cells from whole ileum versus PPs, etc.), it is likely that the recruitment of DCs in mice and pigs is similar.

By the immunohistochemical analysis of intestinal PPs we

found that, after RV infection, the DCs are redistributed toward the SED in a time-dependent manner, which is most evident at 48 h p.i. Redistribution in the SED has been reported previously for intestinal aggregated lymphoid follicles of calves infected with RV (45). The recruitment of DCs toward the SED would allow these cells to capture the RV antigen delivered by M cells from the intestinal lumen, inducing the activation of the distinct subpopulations of DCs. The mobilization of PP DCs also has been described in other murine antigen models. Oral cholera toxin has been reported to induce a very rapid mobilization of immature PP DCs toward the SED (1). It was suggested that this mobilization was induced by the production of CCL20 in the gut. It recently has been shown that CCL20 is produced by intestinal epithelial cells and attracts immature blood-derived DCs *in vitro* in response to *Salmonella enterica* serovar Typhi flagellin (42). The migration of DCs is mediated by the molecule CCL20 and its receptor CCR6, which is present mainly in the IFR DCs. In CCR6-deficient mice, the DCs are absent from the SED of PPs and have an increased number of T cells in the gut-associated lymphoid tissue. Additionally, it was found that there was a deficient intestinal IgA response as well as a delayed clearance of the virus in RV-challenged mice (12). Therefore, the migration of DCs to the SED is important for IgA induction and T-cell homeostasis in the mucosa of the small intestine. Accordingly, we found by flow cytometry that the total DCs from the PPs at 48 h p.i. showed a small but detectable increase of the CCR6 MFI. Taken together, these findings show that DC migration to the SED is important for both T-cell and B-cell responses in intestinal infections.

The efficient activation of T cells by DCs requires three main events: (i) the T-cell recognition of the processed antigen in the context of MHC, (ii) T cells binding to costimulatory molecules expressed by activated DCs (CD40, CD80, and CD86) through CD40L and CD28, and (iii) the secretion of cytokines by DCs (19). Analysis by the flow cytometry of $CD11c^+$ MHC-II^+ DCs cells from PPs at 24 and 48 h p.i. showed a time-dependent increase in the surface expression of the activation markers CD40, CD80, and CD86, correlating well with the observed redistribution of DCs toward the SED that occurs in the same time frame. These findings suggest that some of the DCs return to the T-cell-rich interfollicular regions for the presentation of the antigen to naive lymphocytes. While this study did not test the ability of DCs to present RV antigens to T cells, it has been demonstrated in mice infected with reovirus (14) and *S. enterica* serovar Typhimurium (39).

The mobilization and activation of PP DCs were dependent on viral replication, since DCs from PPs of mice inoculated with UV-treated virus did not show any of these responses during the first 48 h p.i., which correlates well with the failure to detect RV antigen in feces. This result indicates that the viral replication itself as well as the increase of viral load are necessary for the activation of DCs. Further experiments are necessary to dissect the contribution of both factors.

The analysis of purified PP DCs (90% $CD11c^+$ MHC-II^+) from infected mice showed an increase in mRNA expression for the proinflammatory cytokines TNF-α, IL-12/23p40, and IFN-β, as well as for the regulatory cytokine IL-10. The upregulation of mRNA for IFN-β and IL-12/23p40 was found exclusively in the $CD11c^+$ cells, as the $CD11c^-$ cells did not show any detectable increase in mRNA for these cytokines. This finding agrees with previous studies that have shown that DCs are the major producers of IL-12 and type I IFNs (11, 40). On the other hand, both $CD11c^+$ and $CD11c^-$ cells had an increase in mRNA for IL-10 and TNF-α after infection. However, levels were higher in the $CD11c^+$ cells than in $CD11c^-$ cells (19-fold versus 7-folds for IL-10 and 7-fold versus 2.5-fold for TNF-α, respectively). Thus, although we cannot discard that the residual cells (about 10%) present in the purified $CD11c^+$ cells contributed to the increment of mRNA observed, this contribution is presumed to be minimal.

The simultaneous upregulation of both types of cytokines could be explained by the response of a distinct subpopulation of DCs. Iwasaki and Kelsall reported that there are subpopulations of DCs with different immunological functions in the dome and the interfollicular areas of PPs (20). The dome-resident DCs that present the phenotype $CD11c^+$ $CD11b^+$ $CD8^-$ produce low levels of IL-12p70 and high levels of IL-10 upon stimulation (19). In contrast, the interfollicular $CD11c^+$ $CD11b^-$ $CD8^+$ DCs and the $CD11c^+$ $CD11b^-$ $CD8^-$ DCs present in both the dome and the interfollicular region produce mainly type I IFN and IL-12. Consequently, in RV infection, the dome-resident DCs may be the main source of IL-10 and the migrating DCs the source of TNF-α, IL-12/23p40, and IFN-β. On the other hand, the possible role of the recently described plasmacytoid dendritic cells (pDC) of PPs should not be discarded (11), as they have been shown to secrete high levels of IL-12 and low levels of IFN-β. Future experiments are necessary to dissect the DCs population responsible for the production of the different cytokines, although it is clear from the results of this study that the overall result of the activation of different populations of DCs from PPs is a proinflammatory response against the RV infection, but this is regulated by an antiinflammatory response. This guarantees an efficient immune protection response without major tissue damage. In any case, based on the DC phenotype reported here, we believe that the cells described are predominantly mDC-like.

Type I IFNs are the key cytokines produced after viral infection and mediate the induction of both the innate immune response and the subsequent development of adaptive immunity. Type I IFNs induce the maturation of DCs by increasing the expression of activation markers such as CD80, CD86, and CD40 and by facilitating the cross-presentation of viral antigens (25, 49). The expression of type I IFNs is transcriptionally regulated through the coordinated activation of transcription factors including IRF3 (expressed in most nucleated cells) and IRF7 (expressed constitutively in pDC) (44). The RV evasion of the innate immune response has been described *in vitro* in infection-permissive epithelial cell lines, fibroblastic cell lines, and DCs (3, 4, 13, 18). It was found that the NSP1 protein present in the cytosol of infected epithelial cells and fibroblasts efficiently blocked the synthesis of IFN-β through the degradation of the IRF3 transcription factor; however, although the DCs were infected, they did not show IRF3 degradation and therefore were able to secrete IFN-β. On the other hand, it has been demonstrated that NSP1 also can degrade IRF7 and reduce the production of IFN-α/β (13). In our *in vivo* model, we found that purified DCs from PPs at 48 h p.i. presented a clear upregulation of IFN-β gene transcription, whereas no induction at all was observed in DCs from control mice. The

upregulation of IFN-β was not a product of direct DC infection, since by cryomicroscopic studies we found that at 48 h after RV administration less than 1% of cells in PPs are infected (see Fig. S2C and D in the supplemental material). Thus, *in vivo*, the degradation of IRF3 and IRF7 by NSP1, and therefore the reduction of type I IFN production, may work mainly in the epithelial cells.

The *in vivo* data presented here showed that after RV infection, the DCs of PPs are activated and therefore may play a role in the early mucosal immune response against this infection. First by contributing to the innate antiviral response and later by coordinating the subsequent T-cell and B-cell responses, which are crucial to contain and terminate the infection. Further studies are required to determine the role of DC subsets from the LP and the MLN in this infection to obtain a more complete panorama of the mucosal immune response.

ACKNOWLEDGMENTS

We thank Elizabeth Mata, Instituto de Biotecnologia, UNAM, and Fernando Romero and Alberto Alsavez, Instituto Nacional de Salud Publica, SSA, for the excellent animal house conditions, Juana Calderon Amador for technical assistance, Susana Lopez and Carlos Arias for kindly providing us with several reagents, and Ernesto Mendez, Eduardo Garcia, and Vianney Ortiz for critical comments.

This work was supported by grants from SEP-CONACYT (2003-C02-42482-Q and 80149) and PROMEP-PIFI (UAEMOR-CA-26), Mexico. D.L.-G. was supported by CONACYT scholarship no. 102187.

We have no competing financial interests.

REFERENCES

1. **Anjuère, F., C. Luci, M. Lebens, D. Rousseau, C. Hervouet, G. Milon, J. Holmgren, C. Ardavin, and C. Czerkinsky.** 2004. In vivo adjuvant-induced mobilization and maturation of gut dendritic cells after oral administration of cholera toxin. J. Immunol. **173:**5103–5111.
2. **Arias, C. F., M. Lizano, and S. Lopez.** 1987. Synthesis in Escherichia coli and immunological characterization of a polypeptide containing the cleavage sites associated with trypsin enhancement of rotavirus SA11 infectivity. J. Gen. Virol. **68:**633–642.
3. **Barro, M., and J. T. Patton.** 2005. Rotavirus nonstructural protein 1 subverts innate immune response by inducing degradation of IFN regulatory factor 3. Proc. Natl. Acad. Sci. USA **102:**4114–4119.
4. **Barro, M., and J. T. Patton.** 2007. Rotavirus NSP1 inhibits expression of type I interferon by antagonizing the function of interferon regulatory factors IRF3, IRF5, and IRF7. J. Virol. **81:**4473–4481.
5. **Berberich, C., J. R. Ramirez-Pineda, C. Hambrecht, G. Alber, Y. A. Skeiky, and H. Moll.** 2003. Dendritic cell (DC)-based protection against an intracellular pathogen is dependent upon DC-derived IL-12 and can be induced by molecularly defined antigens. J. Immunol. **170:**3171–3179.
6. **Blutt, S. E., C. D. Kirkwood, V. Parreno, K. L. Warfield, M. Ciarlet, M. K. Estes, K. Bok, R. F. Bishop, and M. E. Conner.** 2003. Rotavirus antigenaemia and viraemia: a common event? Lancet **362:**1445–1449.
7. **Blutt, S. E., D. O. Matson, S. E. Crawford, M. A. Staat, P. Azimi, B. L. Bennett, P. A. Piedra, and M. E. Conner.** 2007. Rotavirus antigenemia in children is associated with viremia. PLoS Med. **4:**e121.
8. **Blutt, S. E., K. L. Warfield, D. E. Lewis, and M. E. Conner.** 2002. Early response to rotavirus infection involves massive B cell activation. J. Immunol. **168:**5716–5721.
9. **Burns, J. W., A. A. Krishnaney, P. T. Vo, R. V. Rouse, L. J. Anderson, and H. B. Greenberg.** 1995. Analyses of homologous rotavirus infection in the mouse model. Virology **207:**143–153.
10. **Burns, J. W., M. Siadat-Pajouh, A. A. Krishnaney, and H. B. Greenberg.** 1996. Protective effect of rotavirus VP6-specific IgA monoclonal antibodies that lack neutralizing activity. Science **272:**104–107.
11. **Contractor, N., J. Louten, L. Kim, C. A. Biron, and B. L. Kelsall.** 2007. Cutting edge: Peyer's patch plasmacytoid dendritic cells (pDCs) produce low levels of type I interferons: possible role for IL-10, TGFbeta, and prostaglandin E2 in conditioning a unique mucosal pDC phenotype. J. Immunol. **179:**2690–2694.
12. **Cook, D. N., D. M. Prosser, R. Forster, J. Zhang, N. A. Kuklin, S. J. Abbondanzo, X. D. Niu, S. C. Chen, D. J. Manfra, M. T. Wiekowski, L. M. Sullivan, S. R. Smith, H. B. Greenberg, S. K. Narula, M. Lipp, and S. A. Lira.** 2000. CCR6 mediates dendritic cell localization, lymphocyte homeostasis, and immune responses in mucosal tissue. Immunity **12:**495–503.
13. **Douagi, I., G. M. McInerney, A. S. Hidmark, V. Miriallis, K. Johansen, L. Svensson, and G. B. Karlsson Hedestam.** 2007. Role of interferon regulatory factor 3 in type I interferon responses in rotavirus-infected dendritic cells and fibroblasts. J. Virol. **81:**2758–2768.
14. **Fleeton, M. N., N. Contractor, F. Leon, J. D. Wetzel, T. S. Dermody, and B. L. Kelsall.** 2004. Peyer's patch dendritic cells process viral antigen from apoptotic epithelial cells in the intestine of reovirus-infected mice. J. Exp. Med. **200:**235–245.
15. **Franco, M. A., N. Feng, and H. B. Greenberg.** 1996. Rotavirus immunity in the mouse. Arch. Virol. Suppl. **12:**141–152.
16. **Franco, M. A., and H. B. Greenberg.** 1999. Immunity to rotavirus infection in mice. J. Infect. Dis. **179**(Suppl. 3)**:**S466–S469.
17. **Franco, M. A., C. Tin, L. S. Rott, J. L. VanCott, J. R. McGhee, and H. B. Greenberg.** 1997. Evidence for CD8+ T-cell immunity to murine rotavirus in the absence of perforin, fas, and gamma interferon. J. Virol. **71:**479–486.
18. **Istrate, C., I. Douagi, A. Charpilienne, G. M. McInerney, A. Hidmark, K. Johansen, M. Larsson, K. E. Magnusson, D. Poncet, L. Svensson, and J. Hinkula.** 2007. Bone marrow dendritic cells internalize live RF-81 bovine rotavirus and rotavirus-like particles (RF 2/6-GFP-VLP and RF 8*2/6/7-VLP) but are only activated by live bovine rotavirus. Scand. J. Immunol. **65:**494–502.
19. **Iwasaki, A.** 2007. Mucosal dendritic cells. Annu. Rev. Immunol. **25:**381–418.
20. **Iwasaki, A., and B. L. Kelsall.** 2001. Unique functions of CD11b+, CD8 alpha+, and double-negative Peyer's patch dendritic cells. J. Immunol. **166:**4884–4890.
21. **Johansson, C., and B. L. Kelsall.** 2005. Phenotype and function of intestinal dendritic cells. Semin. Immunol. **17:**284–294.
22. **Krüger, T., D. Benke, F. Eitner, A. Lang, M. Wirtz, E. E. Hamilton-Williams, D. Engel, B. Giese, G. Muller-Newen, J. Floege, and C. Kurts.** 2004. Identification and functional characterization of dendritic cells in the healthy murine kidney and in experimental glomerulonephritis. J. Am. Soc. Nephrol. **15:**613–621.
23. **Kuklin, N. A., L. Rott, J. Darling, J. J. Campbell, M. Franco, N. Feng, W. Muller, N. Wagner, J. Altman, E. C. Butcher, and H. B. Greenberg.** 2000. Alpha(4)beta(7) independent pathway for CD8(+) T cell-mediated intestinal immunity to rotavirus. J. Clin. Investig. **106:**1541–1552.
24. **Kushnir, N., N. A. Bos, A. W. Zuercher, S. E. Coffin, C. A. Moser, P. A. Offit, and J. J. Cebra.** 2001. B2 but not B1 cells can contribute to CD4+ T-cell-mediated clearance of rotavirus in SCID mice. J. Virol. **75:**5482–5490.
25. **Lien, E., and D. T. Golenbock.** 2003. Adjuvants and their signaling pathways: beyond TLRs. Nat. Immunol. **4:**1162–1164.
26. **López, S., and C. F. Arias.** 2004. Multistep entry of rotavirus into cells: a Versaillesque dance. Trends Microbiol. **12:**271–278.
27. **Matsumoto, M., K. Funami, M. Tanabe, H. Oshiumi, M. Shingai, Y. Seto, A. Yamamoto, and T. Seya.** 2003. Subcellular localization of Toll-like receptor 3 in human dendritic cells. J. Immunol. **171:**3154–3162.
28. **McNeal, M. M., M. N. Rae, and R. L. Ward.** 1997. Evidence that resolution of rotavirus infection in mice is due to both CD4 and CD8 cell-dependent activities. J. Virol. **71:**8735–8742.
29. **Mesa, M. C., L. S. Rodriguez, M. A. Franco, and J. Angel.** 2007. Interaction of rotavirus with human peripheral blood mononuclear cells: plasmacytoid dendritic cells play a role in stimulating memory rotavirus specific T cells in vitro. Virology **366:**174–184.
30. **Narváez, C. F., J. Angel, and M. A. Franco.** 2005. Interaction of rotavirus with human myeloid dendritic cells. J. Virol. **79:**14526–14535.
31. **Niedergang, F., and J. P. Kraehenbuhl.** 2000. Much ado about M cells. Trends Cell Biol. **10:**137–141.
32. **Niedergang, F., and M. N. Kweon.** 2005. New trends in antigen uptake in the gut mucosa. Trends Microbiol. **13:**485–490.
33. **Niess, J. H., and H. C. Reinecker.** 2006. Dendritic cells in the recognition of intestinal microbiota. Cell Microbiol. **8:**558–564.
34. **Niess, J. H., and H. C. Reinecker.** 2005. Lamina propria dendritic cells in the physiology and pathology of the gastrointestinal tract. Curr. Opin. Gastroenterol. **21:**687–691.
35. **Parashar, U. D., C. J. Gibson, J. S. Bresse, and R. I. Glass.** 2006. Rotavirus and severe childhood diarrhea. Emerg. Infect. Dis. **12:**304–306.
36. **Pérez-Vargas, J., P. Isa, S. Lopez, and C. F. Arias.** 2006. Rotavirus vaccine: early introduction in Latin America—risks and benefits. Arch. Med. Res. **37:**1–10.
37. **Platt, A. M., and A. M. Mowat.** 2008. Mucosal macrophages and the regulation of immune responses in the intestine. Immunol. Lett. **119:**22–31.
38. **Ruedl, C., C. Rieser, G. Bock, G. Wick, and H. Wolf.** 1996. Phenotypic and functional characterization of CD11c+ dendritic cell population in mouse Peyer's patches. Eur. J. Immunol. **26:**1801–1806.
39. **Salazar-Gonzalez, R. M., J. H. Niess, D. J. Zammit, R. Ravindran, A. Srinivasan, J. R. Maxwell, T. Stoklasek, R. Yadav, I. R. Williams, X. Gu, B. A. McCormick, M. A. Pazos, A. T. Vella, L. Lefrancois, H. C. Reinecker, and S. J. McSorley.** 2006. CCR6-mediated dendritic cell activation of pathogen-specific T cells in Peyer's patches. Immunity **24:**623–632.
40. **Sato, A., and A. Iwasaki.** 2005. Peyer's patch dendritic cells as regulators of mucosal adaptive immunity. Cell Mol. Life Sci. **62:**1333–1338.
41. **Sestak, K., M. M. McNeal, A. Choi, M. J. Cole, G. Ramesh, X. Alvarez, P. P.**

Aye, R. P. Bohm, M. Mohamadzadeh, and R. L. Ward. 2004. Defining T-cell-mediated immune responses in rotavirus-infected juvenile rhesus macaques. J. Virol. **78:**10258–10264.
42. **Sierro, F., B. Dubois, A. Coste, D. Kaiserlian, J. P. Kraehenbuhl, and J. C. Sirard.** 2001. Flagellin stimulation of intestinal epithelial cells triggers CCL20-mediated migration of dendritic cells. Proc. Natl. Acad. Sci. USA **98:**13722–13727.
43. **Steinman, R. M., and H. Hemmi.** 2006. Dendritic cells: translating innate to adaptive immunity. Curr. Top. Microbiol. Immunol. **311:**17–58.
44. **Tailor, P., T. Tamura, and K. Ozato.** 2006. IRF family proteins and type I interferon induction in dendritic cells. Cell Res. **16:**134–140.
45. **Torres-Medina, A.** 1984. Effect of rotavirus and/or Escherichia coli infection on the aggregated lymphoid follicles in the small intestine of neonatal gnotobiotic calves. Am. J. Vet. Res. **45:**652–660.
46. **Trombetta, E. S., and I. Mellman.** 2005. Cell biology of antigen processing in vitro and in vivo. Annu. Rev. Immunol. **23:**975–1028.
47. **van den Berg, T. K., and G. Kraal.** 2005. A function for the macrophage F4/80 molecule in tolerance induction. Trends Immunol. **26:**506–509.
48. **Vancott, J. L., M. M. McNeal, A. H. Choi, and R. L. Ward.** 2003. The role of interferons in rotavirus infections and protection. J. Interferon Cytokine Res. **23:**163–170.
49. **Wallet, M. A., P. Sen, and R. Tisch.** 2005. Immunoregulation of dendritic cells. Clin. Med. Res. **3:**166–175.
50. **Ward, R. L., M. M. McNeal, and J. F. Sheridan.** 1990. Development of an adult mouse model for studies on protection against rotavirus. J. Virol. **64:**5070–5075.
51. **Zhang, W., K. Wen, M. S. Azevedo, A. Gonzalez, L. J. Saif, G. Li, A. E. Yousef, and L. Yuan.** 2008. Lactic acid bacterial colonization and human rotavirus infection influence distribution and frequencies of monocytes/macrophages and dendritic cells in neonatal gnotobiotic pigs. Vet. Immunol. Immunopathol. **121:**222–231.
52. **Zhao, X., A. Sato, C. S. Dela Cruz, M. Linehan, A. Luegering, T. Kucharzik, A. K. Shirakawa, G. Marquez, J. M. Farber, I. Williams, and A. Iwasaki.** 2003. CCL9 is secreted by the follicle-associated epithelium and recruits dome region Peyer's patch CD11b+ dendritic cells. J. Immunol. **171:**2797–2803.